Journal of Colloid and Interface Science 350 (2010) 268–274

Contents lists available at ScienceDirect

Journal of Colloid and Interface Science

www.elsevier.com/locate/jcis

Polymeric scaffolds for enhanced stability of melanin incorporated in liposomes

Marli L. Moraes [a,*], Paulo J. Gomes [b], Paulo A. Ribeiro [b], Pedro Vieira [b], Adilson A. Freitas [c], Ralf Köhler [d], Osvaldo N. Oliveira Jr. [e], Maria Raposo [b]

[a] Universidade Federal de São Carlos, Campus Sorocaba, CP 3031, 18043-970 Sorocaba, São Paulo, Brazil
[b] CEFITEC, Departamento de Física, Faculdade de Ciências e Tecnologia, FCT, Universidade Nova de Lisboa, 2829-516 Caparica, Portugal
[c] Centro de Química Estrutural, DEQB/IST, Lisboa, Portugal
[d] Helmholtz Zentrum Berlin für Materialien und Energie, Glienicker Straße 100, 14109 Berlin, Germany
[e] Instituto de Física de São Carlos, Universidade de São Paulo, CP 369, 13560-970 São Carlos, São Paulo, Brazil

ARTICLE INFO

Article history:
Received 6 February 2010
Accepted 16 June 2010
Available online 22 June 2010

Keywords:
Melanin
Liposome
Dipalmitoyl phosphatidyl glycerol (DPPG)
Layer-by-layer films
Fluorescence
Neutron reflectivity

ABSTRACT

The use of melanin in bioinspired applications is mostly limited by its poor stability in solid films. This problem has been addressed here by incorporating melanin into dipalmitoyl phosphatidyl glycerol (DPPG) liposomes, which were then immobilized onto a solid substrate as an LbL film. Results from steady-state and time-resolved fluorescence indicated an increased stability for melanin incorporated into DPPG liposomes. If not protected by liposomes, melanin looses completely its fluorescence properties in LbL films. The thickness of the liposome-melanin layer obtained from neutron reflectivity data was 4.1 ± 0.2 nm, consistent with the value estimated for the phospholipid bilayer of the liposomes, an evidence of the collapse of most liposomes. On the other hand, the final roughness indicated that some of the liposomes had their structure preserved. In summary, liposomes were proven excellent for encapsulation, thus providing a suitable environment, closer to the physiological conditions without using organic solvents or high pHs.

1. Introduction

Melanins are biopolymers appearing in various living organisms, which display properties such as light absorption in a wide spectral range, photoconduction and piezoelectricity, and perform functions including photoprotection, photosensitization, thermal regulation and anti-oxidation [1–5]. With this variety of properties, melanins are now used in treating diseases [6], and in photoactive, electronic devices and biosensors [7]. In some of these applications, it is convenient to immobilize and manipulate melanins in solid films, which is a major stumbling block because melanins are poorly soluble in most common solvents. Strategies to solubilize melanin as in alkaline aqueous solutions and new methods to synthesize melanin have been described [3]. Cast films of melanins have been reported [1,8,9] but the films are normally heterogeneous and poorly reproducible, and this has prompted researchers to manipulate melanins with detergents and other solvents, e.g. dimethyl sulfoxide (DMSO) [1,3,10]. Considerable progress was made recently with melanin from ammonia solution being spin-coated onto solid supports, with its desirable physical and biological properties preserved [11].

The immobilization of biologically-relevant molecules in solid films is essential for a number of biotechnological applications, which has brought film fabrication methods to the forefront of many research areas. With the layer-by-layer (LbL) technique [12], for instance, biomolecules may be immobilized successfully owing to the control at the molecular level and wide choice of template materials. LbL films have been proven excellent for preserving activity of biomolecules even after drying the films [13], which can be largely attributed to the mild conditions prevailing in film fabrication and the fact that entrained water remains in the film structure after drying [14–16]. Many examples exist of the use of LbL films made of biomolecules [17–20] for applications ranging from biosensing [21] to cell growth (and tissue engineering) [22,23].

Here we exploit the LbL method to adsorb melanin incorporated into phospholipid liposomes where the scaffolds are made of polyelectrolytes. The melanin molecules were incorporated into dipalmitoyl phosphatidyl glycerol (DPPG) liposomes, and then immobilized in layer-by-layer (LbL) films [12], onto a solid substrate, alternated either with poly(allyllamine hydrochloride) (PAH) or poly(ethylene imine) (PEI).

2. Materials and methods

2.1. Materials

Synthetic melanin was purchased from Sigma–Aldrich (product number M8631), and incorporated into liposomes of dipalmitoyl phosphatidyl glycerol (DPPG) from Avanti Polar Lipids.

* Corresponding author.
E-mail address: marli@ufscar.br (M.L. Moraes).

0021-9797/$ - see front matter © 2010 Elsevier Inc. All rights reserved.
doi:10.1016/j.jcis.2010.06.043

2.2. Incorporation of melanin into liposomes

The incorporation of melanin into liposomes was performed according to the following procedure: an aliquot of 1 mM DPPG solution in methanol/chloroform (1:9) was mixed in a 0.16 mg/mL solution of melanin in methanol. After dilution, the solutions were mixed and evaporated with nitrogen until a film formed at the walls of the Falcon tube. This film was hydrated with ultrapure water provided by a Millipore system for 2 h. Liposomes were then obtained by extruding this solution in a mini-extruder from Avanti Polar Lipids in a polycarbonate membrane with 50 nm pores. The incorporation and stabilization of melanin in the liposomes was confirmed with Fourier transform infrared (FTIR), and UV–visible spectroscopy, in addition to steady-state and time-resolved fluorescence measurements with a spectrofluorimeter SPEX-Fluorolog 2, model F212I. Cast films were produced by spreading the aqueous solutions of DPPG and DPPG-melanin liposomes onto CaF_2 substrates.

2.3. Layer-by-layer films

LbL films of melanin-containing DPPG liposomes were fabricated by the alternating adsorption with PAH or PEI layers. For this deposition, the quartz substrate was hydrophilized with a 1:1:5 solution of NH_4OH:H_2O_2:H_2O for 10 min at 70 °C, and then with a 1:1:6 solution of HCl:H_2O_2:H_2O for 10 min at 70 °C. The treated substrate was immersed into a PAH or PEI aqueous solution (1 mg/mL) during 3 min for adsorption of the first layer, which was followed by washing in ultrapure water to remove poorly adsorbed polymer molecules. To complete the first bilayer, the one-layer-coated substrate was immersed for 10 min into the melanin-containing liposome solution, after which another washing step was performed. By repeating this procedure, the desired number of PAH (or PEI)/DPPG liposomes-melanin bilayers could be obtained. Film growth was monitored with UV–visible spectroscopy and fluorescence measurements.

2.4. Neutron reflectivity

The thickness and roughness of a DPPG + melanin layer adsorbed onto a template film were obtained from neutron reflectivity measurements, using a neutron wavelength of 4.66 Å and a graphite monochromator and 3He detector performed on the V6 reflectometer facility at the Berlin Neutron Scattering Center (BENSC), Helmholtz Zentrum Berlin für Materialien und Energie (former Hahn-Meitner-Institut). These measurements consisted in obtaining the reflectivity patterns of thin films at the solid/D_2O interface. The experimental setup used in this work is similar to that described by Howse et al. [24] and Steitz et al. [25]. The data were fitted by applying the optical matrix method [26,27] with Parratt32 fitting program [28]. The template films were prepared onto silicon wafers from 10^{-2} M aqueous solutions of poly(ethylene imine) (PEI), poly(allylamine hydrochloride) (PAH) and poly(styrene sulfonate) (PSS). The template layer sequence was PEI/(PSS/PAH)$_5$. The NaCl salt concentration of the PAH and PSS solutions was 1 M. The adsorption period was 30 min for the PEI layer and 20 min for the PAH and PSS layers. Between each adsorption step the wafer + template film was rinsed with ultrapure water. The silicon wafers of $80 \times 50 \times 10$ mm^3 were purchased from Holm Siliciumbearbeitung, Tann, Germany, and cleaned with "piranha" solution containing hydrogen peroxide and sulfuric acid (1:1). The silicon wafers were kept in the piranha solution for 30 min, after which they were exhaustively washed with ultrapure water. To avoid contamination, the wafers were stored in ultrapure water until the sample preparation.

3. Results and discussion

3.1. Incorporation of melanin into liposomes

Fig. 1a shows the FTIR spectra of melanin in a KBr pellet and in a cast film from an aqueous solution on a CaF_2 substrate. The infrared fingerprint spectra region comprises several peaks that are difficult to split by fitting due to the sample polymeric character. However, several peaks may be inferred by fitting with Gaussian functions, which can then be assigned using density-functional calculations of the electronic and vibrational structures in hydroquinonev (HQ), indolequinone (IQ) and semiquinone (SQ) redox forms of 5,6-dihydroxyindolequinone (DHI) [29] and by analyzing the absorption spectrum of 5,6-dihydroxyindole-2-carboxylic acid (DHICA) [30]. While the spectrum for melanin in the pellet is consistent with that expected from the literature [3], also featuring a broad, intense band at 3440 cm^{-1} due to OH groups from water retained in the sample [3], for the film the spectrum is typical of degraded melanin. The band at 3440 cm^{-1} practically disappeared, i.e. water could not be significantly retained in the film, and bands at 2850 and 2970 cm^{-1} appeared, which are assigned to CH_2 and CH_3 groups, respectively. This result points to a rupture in the melanin ring owing to photodegradation after solubilization. As for the cast films obtained from DPPG liposomes, Fig. 1b shows that

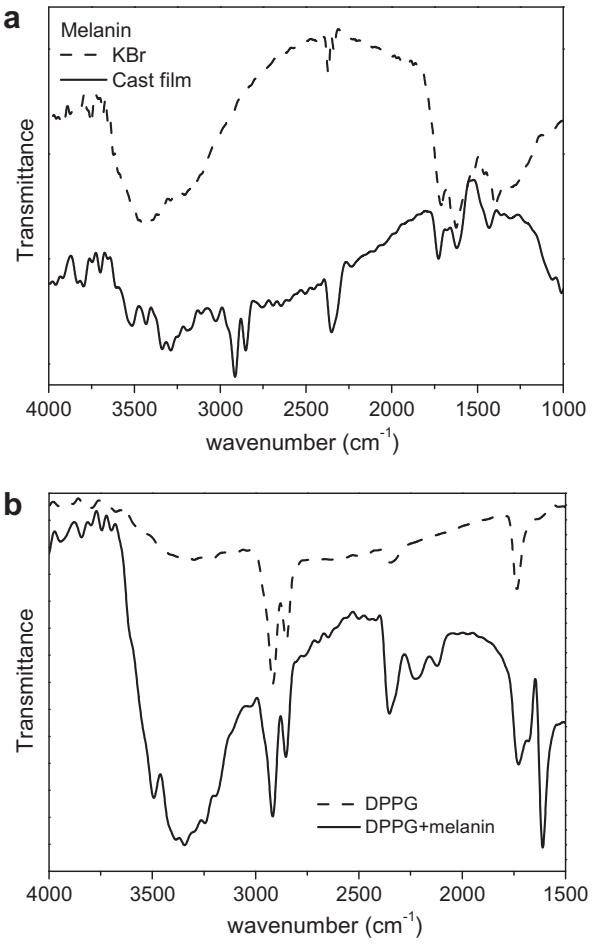

Fig. 1. FTIR spectra for: (a) melanin in KBr pellet (dashed line) and in a cast film (solid line) an0064 (b) cast film obtained with DPPG liposomes (dashed line) and cast film made with melanin-containing DPPG liposomes (solid line). All cast films were deposited onto CaF_2 substrates.

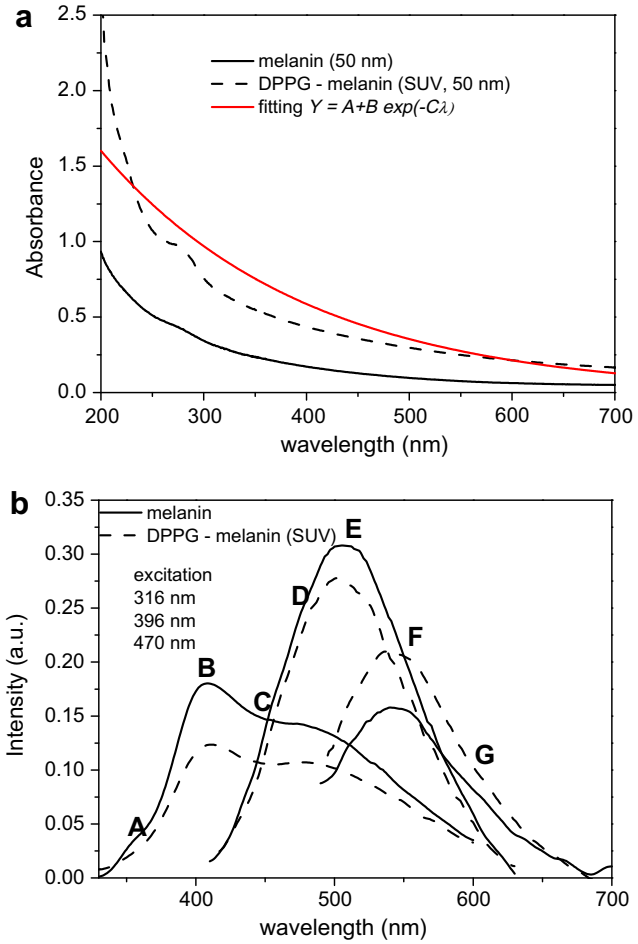

Fig. 2. UV–visible absorption (a) and fluorescence (excitation at 316, 396 and 470 nm) spectra (b) of melanin in ultrapure (Milli-Q) water (solid line) and incorporated into DPPG liposomes (dashed line). Both solutions were extruded with a polycarbonate membrane with 50 nm pores. The peaks identified were marked from A to G.

the band at 3440 cm^{-1} is preserved, being due to OH groups from the DPPG glycerol group and from water retained in the samples. The band is more intense for the film containing melanin, probably because of an additional contribution from OH of melanin without fluorescence properties. The bands at 2850 and 2970 cm^{-1}, assigned to CH_2 and CH_3, respectively, are due to the hydrocarbon chains from DPPG and possibly from melanin without fluorescence properties. Therefore, the incorporation into the liposomes assisted in preserving melanin, though some degradation may not be completely discarded.

With UV–visible spectroscopy one may investigate whether aggregation of melanin occurs. As already mentioned in the introduction, obtaining soluble melanin is crucial for various applications. Fig. 2a shows the absorption spectra for melanin in solution and incorporated into DPPG liposomes, where the long tail extending to large wavelengths is attributed to a distribution of aggregates of various sizes. These spectra were fitted with the function $Y = A + B\exp(-C\lambda)$ described by Miyake et al. [31] for melanin in solution, where Y and λ are the absorption and the wavelength, respectively, and $A = -0.0937$, $B = 4.3643$ and $C = 0.005$ (nm^{-1}). The fitting is ideal when χ^2 is less than 0.00003 which would indicate no *Rayleigh or Mie* light dispersion [2], i.e. the formation of aggregates is minimal. From the spectra in Fig. 2a one infers that a better fitting is obtained with melanin incorporated into DPPG liposomes, and therefore one may conclude that melanin had its solubility enhanced when in liposomes. A small band appears at 280 nm for both solutions, which is related to the melanin used and is also observed for DHICA molecules [32].

The steady-state fluorescence spectra for melanin in solution and in DPPG liposomes are given in Fig. 2b, with excitation being performed at three wavelengths, viz. 316, 396 and 470 nm. Normally, the interaction between a chromophore and liposomes causes a blue shift and a quenching in the spectrum [33], which indeed occurred for the melanin investigated here, with the excitation wavelengths 316 and 396 nm. However, for the sample excited at 470 nm, emission actually increased, which may be due to melanin being exposed, probably in the hydrophilic region of DPPG.

In order to compare these data with the literature, the fluorescence spectra in Fig. 2b were decomposed using Gaussian functions, from which the band position and the full width at half maximum (FWHM) parameters were estimated. The data were fitted with the smaller number of Gaussian peaks that gave the best fits, also imposing that the peak positions should appear in the spectra obtained with different energy excitations. The procedure adopted was as follows. The parameters for the bands obtained with excitation at 470 nm were calculated and used as initial parameters for the determination of band characteristics obtained from excitation at 396 nm. Then, with these latter parameters, those corresponding to the fluorescence bands with excitation at 316 nm were calculated. The results are summarized in Table 1. For the melanin fluorescence curves, C–F, the peaks are positioned at the same wavelengths and with the same peak widths. The same applied to the spectra for DPPG + melanin in curves C, E and F. The values listed in Table 1 were obtained with this systematic search for the number of peaks leading to best fits.

A band centered at 354 nm (peak A) appears only for the melanin solution (not incorporated into liposomes). The bands at 403 nm and at ca. 440 nm can be attributed to the neutral hydrogen bonded and zwitterionic forms, respectively, of the main monomeric unit of melanin, 5,6-dihydroxyindole-2-carboxylic acid (DHICA) [32,34]. The fluorescence spectra of DHICA solutions were shown to depend on the type of solvent, with the emission of the zwitterionic being red-shifted at ~440 nm while the neutral

Table 1
Parameters resulting from fitting the fluorescence spectra of Fig. 2b to Gaussian curves. Seven peaks were identified, being referred to as A through G. Other numbers of peaks were tried, but the fitting with seven peaks was the best one.

Peak	Melanin			Melanin + DPPG		
	Peak position (eV)	Peak position (nm)	Peak width (nm)	Peak position (eV)	Peak position (nm)	Peak width (nm)
A	3.498 ± 0.004	354.5 ± 0.4	16 ± 1	–	–	–
B	3.079 ± 0.002	402.7 ± 0.2	42.9 ± 0.6	3.073 ± 0.002	403.5 ± 0.2	39.2 ± 0.6
C	2.838 ± 0.006	437 ± 1	77.6 ± 0.8	2.85 ± 0.02	435 ± 2	91 ± 3
D	2.67 ± 0.02	464 ± 4	51.0 ± 0.3	–	–	–
E	2.42 ± 0.01	512 ± 2	60.4 ± 0.7	2.528 ± 0.001	490.4 ± 0.2	70.1 ± 0.3
F	2.23 ± 0.01	556 ± 3	39.5 ± 0.5	2.289 ± 0.002	541.6 ± 0.3	83.8 ± 0.6
G	2.10 ± 0.03	591 ± 9	38.9 ± 0.5	1.990 ± 0.003	623 ± 1	58 ± 2

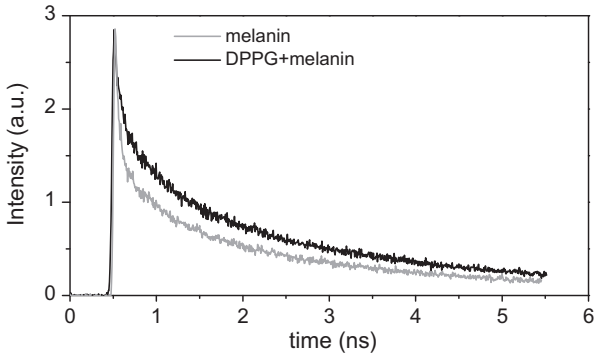

Fig. 3. Fluorescent decay at 525 nm following excitation at 396 nm for melanin in water solution (gray) and in DPPG liposomes (black).

hydrogen bonded form emits at 390–410 nm [32]. Similar results were observed for indole-2-carboxylic acid and indole-5-carboxylic acid [34]. One should bear in mind that the neutral hydrogen bonded and the zwitterionic forms are both present in the same melanin molecule. The areas of peak C of the zwitterionic form are approximately the same for both solutions. However, they are larger than for the hydrogen bond form (peak B) according to a ratio of the areas of the Gaussian of 1.6 and 3.6, for melanin and melanin + DPPG, which points to a lower number of neutral hydrogen bonds in aqueous solutions of melanin + DPPG.

The equilibrium between the excited states of the hydrogen bonded and the zwitterionic forms has been invoked to explain the fluorescence properties of DHICA molecules [32], with emission occurring at ~470 nm for the hydrogen bonded and at ~520 nm for the zwitterionic forms. For the solution of melanin, the fluorescence spectra displayed bands at 464 nm (peak D) and 512 nm (peak E), which are close to the values above [32]. However, these bands are blue shifted by ca. 30 nm for melanin + DPPG solutions, as they appear at 490 nm and 542 nm. The contribution from the zwitterionic form is higher, with ratios between the band areas of 2.9 and 1.7 for melanin and melanin + DPPG aqueous solutions, respectively. Therefore, for the melanin incorporated into DPPG liposomes, a decrease was observed in the excited states of the zwitterionic form owing to the negative charges or the OH groups of the phospholipids.

The fluorescence decays of melanin in solution and in DPPG + melanin liposomes are shown in Fig. 3, for the fluorescence decay monitored at 525 nm following excitation at 396 nm. The decay could be fitted with a multi-exponential function $I(t) = \Sigma_i \alpha_i \exp(-t/\tau)$, where $I(t)$ is the intensity, α_i is a pre-exponential factor and τ_i is the lifetime of specie i. The number of species was chosen so as to obtain the best fitting, with high correlation coefficients and small error bars. The fitting is omitted for it coincides with the experimental curves. The pre-exponential factors and lifetime constants are listed in Table 2, which also includes the values of Forest et al. [35] for eumelanin from *sepia officinalis* obtained with time-resolved emission at 520 nm and excitation at 335 nm. The parameters in Table 2 for the dynamics of the DPPG + melanin solution are similar to those of eumelanin [35] and for bovine and human eye melanins [36], which were non-degraded. In contrast, for non-incorporated melanin in solution, the parameters differed, with a larger contribution from the fast dynamics (lifetime less than 1 ns) associated with aggregated melanin [36]. Therefore, consistent with the UV–visible and steady-state fluorescence spectroscopy results above, melanin is less aggregated when incorporated into liposomes.

The lifetimes τ_2 and τ_3 are close to those of Birch et al. [37] for reversed micelles of melanin prepared by self-oxidation of L-dihydoxyphenylalamine (DOPA) while Ehlers et al. [38] found lifetime constants of 0.04 ns for DOPA melanin in cast films. The lifetime τ_1 of 0.05 ns for DPPG + melanin may indicate a small degree of aggregation in comparison to melanin in water, as the mean lifetime tends to decay with the size of the melanin molecules [37]. In addition, as the particles become larger the fluorescence can be depolarized with lifetime constants <100 ps [36]. The lifetime constants of 0.4 ns can indicate the presence of DHICA monomeric units in the zwitterionic form. Under this condition the protonated COOH group developed HN–HOOC hydrogen bonds that may yield a red-shifted[1] zwitterionic fluorescence [32], which explains the red shift in Fig. 2b for the zwitterionic form.

3.2. Layer-by-layer films containing melanin

LbL films were produced from solutions of melanin in pure water and in DPPG liposomes, alternated with layers of either PAH or PEI. Fig. 4 shows the UV–visible spectra for the LbL films grown with PEI/melanin (Fig. 4a) and PEI/DPPG + melanin (Fig. 4b). Those produced from melanin in an aqueous solution did not display a linear increase in absorbance with the number of bilayers, as can be seen in the inset in Fig. 4a. Saturation of the amount of adsorbed material occurred after only two bilayers had been deposited. Furthermore, the spectra feature a band at 400 nm, which is probably due to degraded melanin [39]. In contrast, the growth of LbL films of PEI with melanin in DPPG liposomes was linear, though there was a change in slope, as indicated in the inset in Fig. 4b. This change may be attributed to a rearrangement or even rupture of liposomes. There was very little adsorption for films with PAH (data not shown), which will no longer be discussed here.

The kinetics of adsorption of a liposome-melanin layer was analyzed by plotting the optical absorption at 396 nm vs. the time of immersion for the film fabrication (result not shown). Growth may be explained with two first-order kinetics processes [40], as follows:

$$A = k_1(1 - \exp(-t/\tau_1)) + k_2(1 - \exp(-(t/\tau_2)) \quad (1)$$

where A is the absorbance at 396 nm, which is assumed proportional to the melanin adsorbed amount, k_1, k_2 represent the maximum adsorbed amount and τ_1 and τ_2 are the characteristic times of each adsorption process. Adsorption tends to saturate above 600 s, thus pointing to the required time for a full layer of liposome-melanin to be adsorbed. The parameters obtained from the fitting of Eq. (1) were $k_1 = 0.030 \pm 0.002$; $\tau_1 = 1.6 \pm 0.8$ s; $k_2 = 0.061 \pm 0.002$ and $\tau_2 = 240 \pm 20$ s. The first process is very fast, being associated with the instantaneous adsorption of liposome + melanin onto the substrate as observed in polyelectrolyte adsorption processes. The second process is associated with diffusion of liposome + melanin that were not initially near the substrate [40,41]. This second process is also related to adsorption of counterions and co-ions to facilitate the adsorption of liposome + melanin.

The structural features of LbL films containing melanin incorporated into liposomes were observed using neutron reflectivity measurements at the solid/D_2O interface. Fig. 5 shows the neutron reflectivity curves for liposome-melanin layers adsorbed onto the template PEI/$(PSS/PAH)_5$ LbL film, the parameters of which have been reported previously [42]. The curves were fitted using the Parratt32 Reflectivity Tool [26,27] using a one-box model and only the first reflectivity fringe. The results for thickness and roughness are listed in Table 3, from which one infers 4.1 ± 0.2 nm and 7.4 ± 1.2 nm for the thickness and roughness of the layer of DPPG + melanin, respectively. This thickness is consistent with that estimated for the phospholipid bilayer of 4.21 nm, obtained as the distance between the phosphorus peaks across the bilayer using

[1] For interpretation of color in Fig. 2, the reader is referred to the web version of this article.

Table 2
Lifetime (τ) and normalized pre-exponential factor (α) for melanin in pure water and in DPPG liposomes. Values for eumelanin from Ref. [35] are given for comparison.

	τ (ns)				α			
	1	2	3	4	1	2	3	4
Melanin in water	0.02	0.41	3.08	–	0.77	0.12	0.11	–
DPPG + melanin	0.05	0.47	2.98	–	0.54	0.21	0.25	–
Eumelanin from [35]	0.06	0.52	2.5	6.9	0.52	0.22	0.19	0.07
Reversed micelles of melanin [37]	–	0.41	1.5	2.7	–	0.17	0.57	0.28

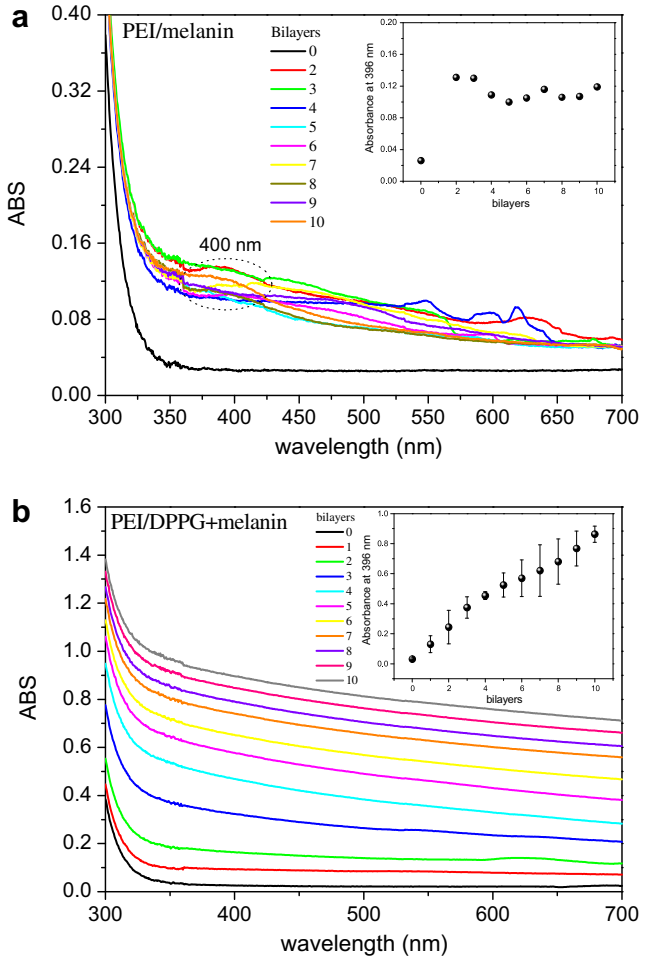

Fig. 4. UV–visible spectra for LbL films with various numbers of bilayers of PEI/melanin (a) and PEI/melanin-containing liposomes (b). Inset: absorption at 396 nm vs. number of bilayers for PEI/melanin (a) and PEI/DPPG-melanin (b).

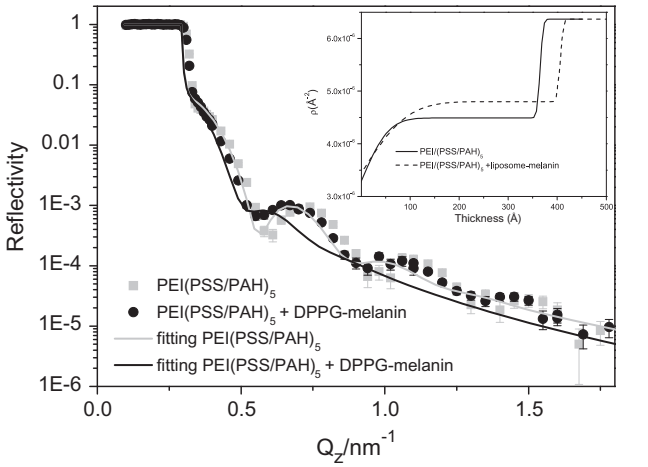

Fig. 5. Neutron reflectivity curves as obtained from the template PEI(PSS/PAH)$_5$ (gray) and PEI(PSS/PAH)$_5$ liposome-melanin films (black). The fittings appear as solid lines. Inset: Scattering length density (ρ) profile from fitting to the neutron reflectivity data. *The discrepancy between the fitting and the experimental data for the LbL film containing liposomes and melanin is due to the fact that only the first reflectivity fringe, considering one-box model, was used to calculate the layer thickness and roughness.*

Table 3
Calculated film thickness (d), roughness (σ) and scattering length density (ρ) obtained from the best fits to the neutron reflectivity data.[a]

	d (Å)	σ (Å)	ρ (Å^{-2})
PEI/(PSS/PAH)$_5$	365 ± 7	44 ± 9	$(4.49 \pm 0.08) \times 10^{-6}$
PEI/(PSS/PAH)$_5$ + liposome-melanin	406 ± 8	74 ± 12	$(4.8 \pm 0.1) \times 10^{-6}$

[a] The one-box model was used throughout the analysis and error bars were set in accordance to a level of 10% increase in χ^2. The scattering length density parameters for silicon and D_2O were kept constant: $\rho_{Si} = 2.07 \times 10^{-6}$ Å^{-2} and $\rho_{D2O} = 6.37 \times 10^{-6}$ Å^{-2}.

simulated electron density profiles [43]. Because the final roughness is near twice the bilayer thickness, one infers that some liposomes did not collapse when adsorbed on the substrate, which may also explain why the fitting in Fig. 5 is not as good as for the films without liposomes.

Another possible reason for the poor fitting in Fig. 5 could be the use of a one-box model and the first reflectivity fringe. We therefore extended our analysis with models with more than one-box, both taking into account the film roughness and disregarding the roughness. In this extended analysis, we noted that the fits without roughness are three times worse than those including roughness. A problem intrinsic in our samples was that the roughness is beyond the limit of 1/3 of the box thickness. Nevertheless, the derivative plot showed an increase in mean thickness after incubation with melanin of +28 Å. The same was true for the 5-box model used without the roughness, which yielded an increase of +27 Å after incubation with melanin. Upon plotting the difference of the real space profiles, we observed that this difference is proportional to the volume fraction of the additional protonated material, i.e. lipids + melanin, centered at a distance from the substrate of 400 Å with a broad distribution of ±82 Å. It is therefore concluded that there is interpenetration of adjacent layers as in other LbL films, which makes it difficult to obtain a good fitting of the reflectivity data.

Melanin appeared to be completely in non-fluorescent form when in LbL films with PEI, with no emission being observed when the films were excited at three wavelengths (316, 396 and 470 nm), thus confirming the results obtained with UV–visible spectroscopy. In contrast, as Fig. 6a shows, melanin had its fluorescence with excitation at 396 nm preserved if immobilized in liposomes in an LbL film with PEI, even after months of film fabrication. The emission peak was slightly shifted (only 2 nm) in comparison with the solution spectrum, which is due to aggregation. Indeed, aggregation appears to occur as indicated by the time-resolved fluores-

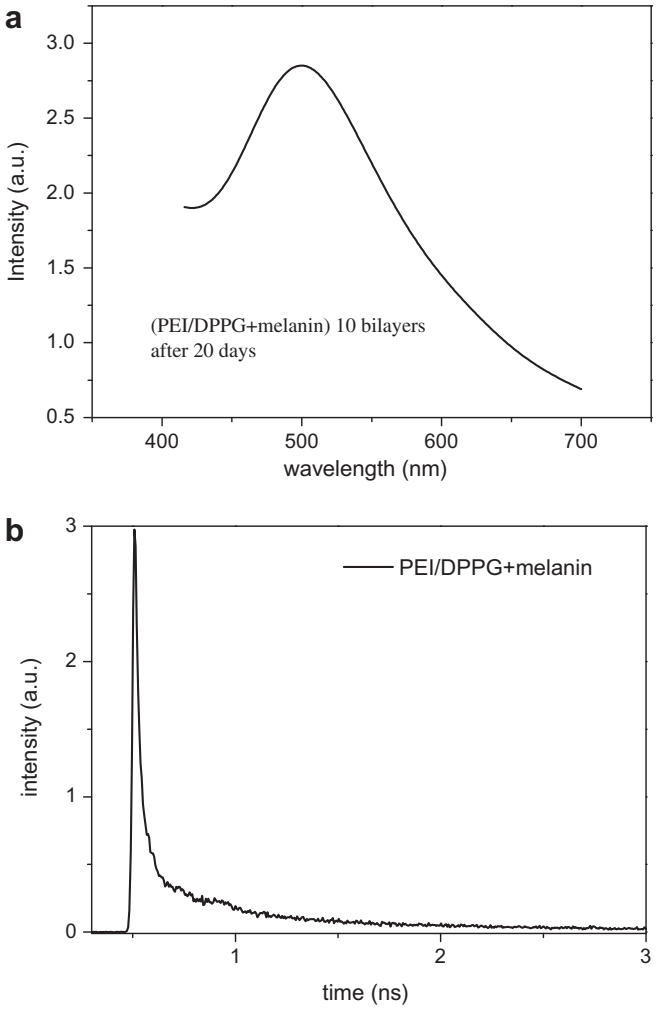

Fig. 6. Emission spectrum for a 10-bilayer PEI/liposome-melanin film (a). Fluorescence decay for the same film (b).

cence measurements depicted in Fig. 6, which shows the fluorescence decay monitored at 525 nm following excitation at 396 nm. The decay of the fast process had a lifetime of 0.01 ns and a pre-exponential factor of 0.9. The large contribution from this process also points to some aggregation of melanin. Nevertheless, melanin emission was still observed, which was preserved even for measurements with the same film several months after fabrication.

4. Conclusions

In this study we demonstrated that melanin may be incorporated into DPPG liposomes and exhibit better solubility and stability than free melanin in an aqueous solution. In addition to being excellent for encapsulation, the liposomes were useful for melanin to keep its activity, as demonstrated with fluorescence measurements. This achievement is significant insofar as the liposomes provide an environment that is closer to the physiological conditions, and there was no need to employ organic solvents to stabilize melanins. Finally, the incorporation of melanin had little effect on the structuring of DPPG liposomes, as indicated in neutron reflectivity studies.

One of the most important functions of melanin is in photoprotection as it strongly absorbs UV light and has efficient non-radiactive dissipation of the absorbed energy. Therefore, the fabrication of melanin films, especially if incorporated in a biomimetic material as has been done here, may be relevant for radiation damage studies [44]. Furthermore, it is important to understand how melanin behaves biochemically, since melanin has been associated to the immune system [45,46] and for protection against Parkinson's disease [47,48].

Acknowledgments

The authors acknowledge the financial support from Capes/Grices (Bex0159/07-7), FAPESP and CNPq (Brazil), from project **"X-rays and UV effects on Biomimetic Membranes"** (PHY-04-1418) to Access to Research Infrastructures, Berlin Neutron Scattering, (Germany) and from "Fundação para a Ciência e Tecnologia" (Portugal).

References

[1] C.M.R. Clancy, J.B. Nofsinger, R.K. Hanks, J.D. Simon, J. Phys. Chem. B 104 (2000) 7871.
[2] P. Díaz, Y. Gimeno, P. Carro, S. González, P.L. Schilardi, G. Benítez, R.C. Salvarezza, A.H. Creus, Langmuir 21 (2005) 5924.
[3] M.I.N. da Silva, S.N. Dezidério, J.C. Gonzalez, C.F.O. Graeff, M.A.J. Cotta, Appl. Phys. 96 (2004) 5803.
[4] A.B. Mostert, K.J.P. Davy, J.L. Ruggles, B.J. Powell, I.R. Gentle, P. Meredith, Langmuir 26 (2010) 412.
[5] A.A.R. Watt, J.P. Bothma, P. Meredith, Soft Matter. 5 (2009) 3754.
[6] Y.C. Hung, V.M. Sava, V.A. Blagodarsky, M.-Y. Hong, G.S. Huang, Life Sci. 72 (2003) 1061.
[7] A.M. Karlsson, K. Bjuhr, M. Testorf, P.Å. Öberg, E. Lerner, I. Lundström, S.P.S. Svensson, Biosens. Bioelectron. 17 (2002) 331.
[8] G.S. Lorite, V.R. Coluci, M.I.N. da Silva, S.N. Dezidério, C.F.O. Graeff, D.S. Galvão, M.A. Cotta, J. Appl. Phys. 99 (2006) 113511.
[9] M. Abbas, F. D'Amico, L. Morresi, N. Pinto, M. Ficcadenti, R. Natali, L. Ottaviano, M. Passacantando, M. Cuccioloni, M. Angeletti, R. Gunnella, Eur. Phys. J. E 28 (2009) 285.
[10] Y.V. Il'ichev, J.D. Simon, J. Phys. Chem. B 107 (2003) 7162.
[11] J.P. Bothma, J. de Boor, U. Divakar, P.E. Schwenn, P. Meredith, Adv. Mater. 20 (2008) 3539.
[12] G. Decher, Science 277 (1997) 1232.
[13] Y. Lvov, K. Ariga, I. Ichinose, T. Kunitake, Thin Solid Films 284 (1996) 797.
[14] J.M.C. Lourenço, P.A. Ribeiro, A.M. Botelho do Rego, F.M. Braz Fernandes, A.M.C. Moutinho, M. Raposo, Langmuir 20 (2004) 8103.
[15] J.M.C. Lourenço, P.A. Ribeiro, A.M. Botelho do Rego, M. Raposo, J. Colloid Interface Sci. 313 (2007) 26.
[16] Y. Lvov, A. Katsuhiko, I. Ichinose, T. Kunitake, J. Am. Chem. Soc. 117 (1995) 6117.
[17] K. Ariga, T. Nakanishi, T. Michinobu, J. Nanosci. Nanotechnol. 6 (2006) 2278.
[18] A.P.R. Johnston, C. Cortez, A.S. Angelatos, F. Caruso, Curr. Opin. Colloid Interface Sci. 11 (2006) 203.
[19] K. Ariga, J.P. Hill, Q. Ji, Phys. Chem. Chem. Phys. 9 (2007) 2319.
[20] K. Ariga, J.P. Hill, M.V. Lee, A. Vinu, R. Charvet, S. Acharya, Sci. Technol. Adv. Mater. 9 (2008) 014109.
[21] M.L. Moraes, U.P. Rodrigues Filho, O.N. Oliveira Jr., M. Ferreira, J. Solid State Electrochem. 11 (2007) 1489.
[22] Y. Liu, T. He, H. Song, C. Gao, J. Biomed. Mater. Res. A 81 (2007) 692.
[23] Z. Tang, Y. Wang, P. Podsiadlo, N.A. Kotov, Adv. Mater. 18 (2006) 3203.
[24] J.R. Howse, E. Manzanares-Papayanopolous, I.A. McLure, J. Bowers, R. Steitz, G.H. Findenegg, J. Chem. Phys. 116 (2002) 7177.
[25] R. Steitz, V. Leiner, R. Siebrecht, R. von Klitzing, Colloids Surface A 163 (2000) 63.
[26] L.G. Parratt, Phys. Rev. 95 (1954) 359.
[27] T.P. Russell, Mater. Sci. Rep. 5 (1990) 171.
[28] C. Braun, PARRATT 32 Program, Berlin Neutron Scattering Center (BENSC), Hahn-Meitner Institut, 1997–2002.
[29] B.J. Powell, T. Baruah, N. Bernstein, K. Brake, R.H. MacKenzie, P. Meredith, M.R. Pederson, J. Chem. Phys. 120 (2004) 8608.
[30] H. Okuda, A. Nakamura, K. Wakamatsu, S. Ito, T. Sota, Chem. Phys. Lett. 433 (2007) 355.
[31] Y. Miyake, Y. Izumi, A. Tsutsume, K. Jimbow, Structure and Function of Melanin, Fuji-shoin, Sapporo, 1986.
[32] M. Gauden, A. Pezzella, L. Panzella, M.T. Neves-Petersen, E. Skovsen, S.B. Peterse, K.M. Mullen, A. Napolitano, M. d'Ischia, V. Sundström, J. Am. Chem. Soc. 130 (2008) 17038.
[33] J.R. Lakowicz, Principles of Fluorescence Spectroscopy, Springer, 2006.
[34] P.R. Banga, S. Chakravorti, J. Phys. Chem. A 103 (1999) 8585.
[35] S.E. Forest, W.C. Lam, D.P. Millar, J.B. Nofsinger, J.D. Simon, J. Phys. Chem. B 104 (2000) 811.
[36] J.B. Nofsinger, J.D. Simon, Photochem. Photobiol. 74 (2001) 31.
[37] D.J.S. Birch, A. Ganesan, J. Karolin, Synth. Met. 155 (2005) 410.

[38] A. Ehlers, I. Riemann, M. Stark, K. König, Microsc. Res. Tech. 70 (2007) 154.
[39] P. Kayatz, G. Thumann, T.T. Luther, J.F. Jordan, K.U. Bartz-Schmidt, P.J. Esser, U. Schraermeyer, IOVS 42 (2001) 241.
[40] M. Raposo, R.S. Pontes, L.H.C. Mattoso, O.N. Oliveira Jr., Macromolecules 30 (1997) 6095.
[41] M. Raposo, O.N. Oliveira Jr., Langmuir 16 (2000) 2839.
[42] P.A. Ribeiro, R. Steitz, I.E. Lopis, H. Haas, N.C. Souza, O.N. Oliveira Jr., M. Raposo, J. Nanosci. Nanotechnol. 6 (2006) 1396.
[43] T. Zaraiskaya, K.R. Jeffrey, Biophys. J. 88 (2005) 4017.
[44] M. Raposo, P.J. Gomes, J.M.C. Lourenço, M. Coelho, S.V. Hoffmann, A.M. Botelho do Rego, R.W. McCullough, N.J. Mason, C. Lage, P. Limão-Vieira, P.A. Ribeiro, AIP Conf. Proc. 1080 (2008) 125.
[45] J.A. Mackintosh, J. Theor. Biol. 211 (2001) 101.
[46] C.G. Burkhart, C.N. Burkhart, Int. J. Dermatol. 44 (2005) 340.
[47] K. Wakamatsu, K. Fujikawa, F.A. Zucca, L. Zecca, S. Ito, J. Neurochem. 86 (2003) 1015.
[48] M. Sasaki, E. Shibata, K. Tohyama, J. Takahashi, K. Otsuka, K. Tsuchiya, S. Takahashi, S. Ehara, Y. Terayama, A. Sakai, Neuroreport 17 (2006) 1215.